Available online at www.sciencedirect.com
ScienceDirect
Cement & Concrete Composites 29 (2007) 656–666
Cement & Concrete Composites
www.elsevier.com/locate/cemconcomp

Electrical conductivity based characterization of plain and coarse glass powder modified cement pastes

Nathan Schwarz, Matthew DuBois, Narayanan Neithalath *

Department of Civil and Environmental Engineering, Clarkson University, Potsdam, NY 13699, USA

Received 29 August 2006; received in revised form 28 March 2007; accepted 4 May 2007
Available online 18 May 2007

Abstract

This paper describes the use of electrical conductivity to characterize plain and coarse glass powder modified cement pastes. It is observed that the glass powder addition facilitates improved hydration of the cement grains. For the proportions investigated in this study, and the particle size of glass powder, this advantage is negated by the reduced amount of hydration products, i.e., the dilution effect. The variation of electrical conductivity and its derivative with time can be related to the various phases in the microstructural development of the paste. It is observed from the time derivative of conductivity plots that the addition of glass powder results only in minor changes in the setting time of the pastes. Higher the glass powder content, higher the normalized conductivity (ratio of conductivity at a certain glass powder content to that of plain paste) at very early times, and then it falls to a value closer to or less than 1.0 at later times. A parallel model is used to represent effective conductivity as a function of the pore solution conductivity, porosity, and pore connectivity factor. The pore solution conductivity increases with increase in glass powder content. The porosity of the pastes reduces with increase in glass powder content at early ages and increases at later ages. A reduced pore connectivity factor is observed for pastes with higher glass powder content at later times. However, this does not imply increased volume of hydration products as is commonly interpreted for normal pastes, but the electrical conduction pathways are made more tortuous by the relatively large volume of un-reacted filler material in the pore structure.

Keywords: Hydration; Characterization; Microstructure; Electrical properties; Cement paste; Glass powder; Porosity; Pore connectivity factor

1. Introduction

The use of high performance concrete (HPC) and self-consolidating concrete (SCC) have gained prominence in global concrete construction. These concretes are proportioned with a substantially reduced water–cement ratio (w/c) and incorporate a variety of additives. With a reduced w/c, it is well known that not all the cement in the concrete mixture participates in hydration reactions, and for w/c less than 0.38, some unhydrated cement remain in the system [1]. In order to ensure more efficient usage of energy and materials, it has been suggested that coarser cements be used in HPC [2], or the coarser cement particles that will not undergo complete hydration in low w/c mixtures be replaced by inert filler materials like ground sand or limestone powder [3,4]. The addition of limestone powder to cement is common in Europe and up to 35% of limestone powder can be added to produce portland limestone cement [5]. In the United States, ASTM C150, the standard specification for portland cement allows limestone additions of up to 5%. The limestone filler improves the dispersion of cement grains and thus the hydration rate of cement [6]. Other inert filler materials that can be used in HPC and SCC are glass powder, stone dust, and chalk powder [5,7,8].

This paper examines the influence of waste glass powder as filler on the properties of cement pastes. The recycling of waste glass is a major problem in large municipal areas of developed countries [9,10]. In regions where there are local

* Corresponding author. Tel.: +1 315 268 1261; fax: +1 315 268 7985.
E-mail address: nneithal@clarkson.edu (N. Neithalath).

0958-9465/$ - see front matter © 2007 Elsevier Ltd. All rights reserved.
doi:10.1016/j.cemconcomp.2007.05.005

sources of glass powder, either from the crushing of post consumer glass or from the production of industrial application and highway safety glass beads, which needs to be safely disposed, their use in concrete becomes an environment-friendly option. A few studies have reported the use of waste glass as a raw siliceous material for the production of portland cement [11,12], but the concerns with high alkali content remain. Previous studies on the use of glass powder [7,10,13,14] have investigated the pozzolanicity and strength development of mortars and concrete incorporating fine glass powder, whereas this study employs electrical property based methods to characterize cement pastes in which a coarser glass powder is used as filler. Characterizing such non-conventional materials with respect to their behavior in cementitious systems is an important step that is expected to lead to (i) better confidence in the usage of such materials in concrete, thus leading to sustainable methods of waste utilization, and (ii) the selection of optimal dosages of these replacement materials.

2. Experimental program

2.1. Materials and mixtures

Type I ordinary portland cement conforming to ASTM C 150 is used for the cement pastes investigated in this study. The glass powder was obtained from Potters Industries, Potsdam, NY, a manufacturer of highway safety glass spheres and industrial glass beads. The waste glass powder from this facility comes in two different particle size distributions – a coarser powder with 60% finer than 88 μm, and a finer variety with 90% finer than 45 μm. The glass powder used in this study was the coarser of the two since it is used just as filler. Cement pastes were prepared with two different water-solids (cement + glass powder) ratios (w/s) of 0.32 and 0.42. The replacement rates of cement with glass powder were 10%, 20%, and 30% by mass. The physical characteristics and chemical composition of the cement and glass powder are shown in Table 1. Fig. 1 shows a micrograph of the glass powder along with the energy dispersive X-ray spectrum (EDX) indicating the dominant elements.

Table 1
Chemical composition and physical characteristics of cement and glass powder

Composition (% by mass)/property	Cement	Glass powder
Silica (SiO_2)	20.2	72.5
Alumina (Al_2O_3)	4.7	0.4
Iron oxide (Fe_2O_3)	3.0	0.2
Calcium oxide (CaO)	61.9	9.7
Magnesium oxide (MgO)	2.6	3.3
Sodium oxide (Na_2O)	0.19	13.7
Potassium oxide (K_2O)	0.82	0.1
Sulfur trioxide (SO_3)	3.9	–
Loss on ignition	1.9	–
Fineness, % passing (sieve size)	97.4 (45 μm)	60 (88 μm)
Specific surface area (m^2/kg)	388	262
Density (kg/m^3)	3150	2490

Cement and glass powder were mixed dry in a laboratory mortar mixer for 2 min. Water was then gradually added and mixed for further 3 min. After the mixing time, a part of the mixture was filled in acrylic molds for electrical property measurements, another part filled in 50 mm cube molds for compressive strength test at various ages, and another part used for flow table tests to determine workability as per ASTM C 1437.

2.2. Electrical impedance spectroscopy (EIS) for conductivity determination

Electrical impedance spectroscopy tests on the cement pastes were carried out using a HP 4284A LCR meter connected to a personal computer for data acquisition. The cement pastes were filled in acrylic molds (50 mm × 50 mm × 150 mm) immediately after they were mixed. Two stainless steel plates (50 mm × 75 mm × 0.75 mm) were placed at the ends of the molds to be used as electrodes. Alligator plugs from the impedance analyzer were attached to the electrodes. The impedance measurements were carried out over a frequency range of 20 Hz to 1 MHz at five measurements a decade, using a 250 mV AC signal. A typical Nyquist plot (plot of real versus imaginary impedance) obtained from EIS measurements consists of two arcs – the bulk arc and the electrode arc. The two arcs meet at a point where the imaginary component of the impedance is minimum, and the corresponding real impedance is the bulk resistance (R_b) of the sample. The effective conductivity (σ_{eff}) is calculated from the bulk resistance as

$$\sigma_{eff} = \frac{l}{R_b A} \tag{1}$$

where l is the specimen length, and A is the cross-sectional area.

2.3. Non-evaporable water content and degree of hydration

Non-evaporable water content (w_n) is used in this paper as a measure of the degree of hydration of cement pastes. Small pieces of pastes (2–4 g in mass) were cured in completely saturated conditions at 20 °C. At different ages (1, 3, 7, 14, and 28 days), the hardened pastes were removed from water, crushed into powder, and flushed with acetone to stop further hydration. The samples were placed in crucibles and heated to 105 ± 5 °C for 24 h in an oven. After the 24 h period, the crucibles were weighed (w_{105}) and then kept in a muffle furnace at 1050 °C for 3 h, after which they were allowed to cool to ambient temperature in a dessicator and weighed (w_{1050}). Non-evaporable water content (w_n) is obtained as

$$w_n = \frac{w_{105} - w_{1050}}{w_{1050}} \tag{2}$$

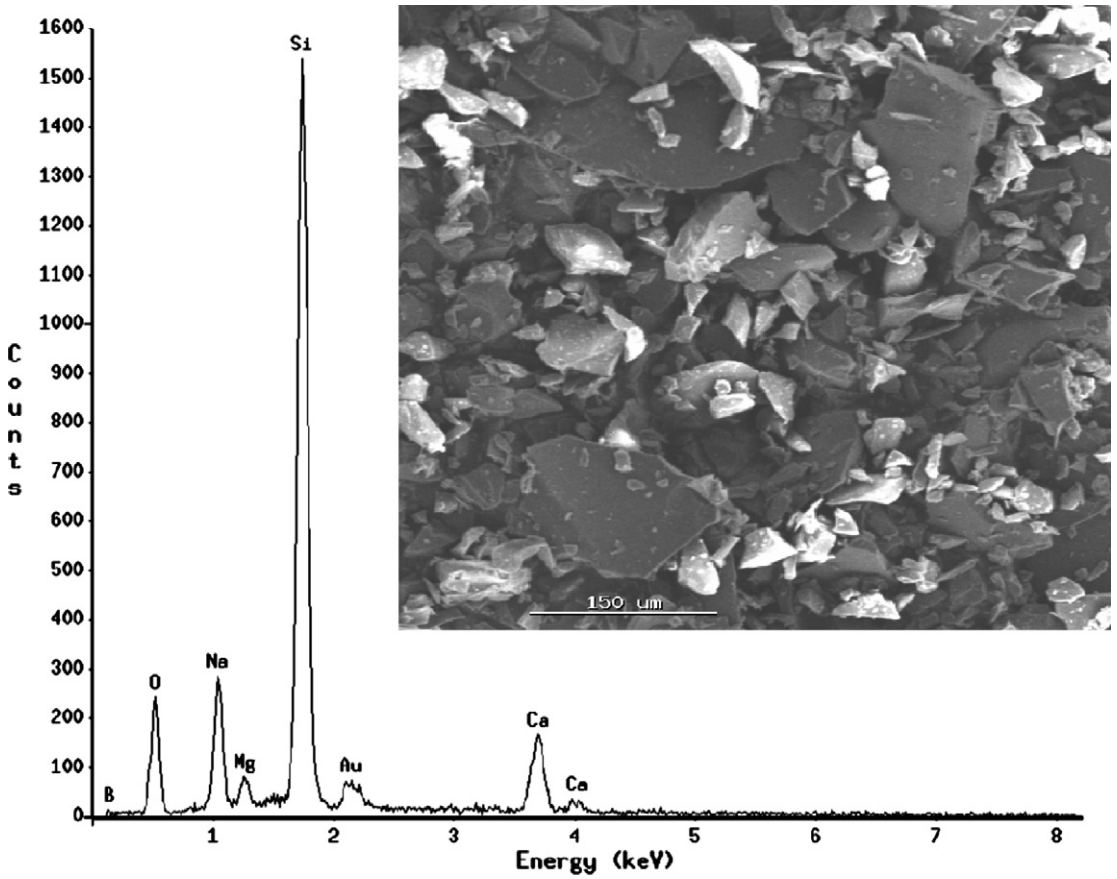

Fig. 1. SEM image and EDX analysis of the glass powder used in this study.

The w_n values of plain pastes were converted into degrees of hydration (α) by dividing them with the w_n of a completely hydrated paste, which is 0.24, and subtracting the loss of ignition of the dry cement. Since the glass powder is only a filler, the obtained degrees of hydration of modified pastes were corrected using the mass fraction of cement in the mixtures to give actual degrees of hydration (α_{act})

$$\alpha_{act} = \mathrm{Min}\left\{1, \frac{\alpha}{(1 - g/100)}\right\} \quad (3)$$

where g is the percentage of glass powder replacing cement. The minimum function is used to pre-empt the possibility of α_{act} attaining values greater than 1.0.

3. Results, analysis and discussions

3.1. Flow behavior and compressive strength of modified pastes

The workability of the plain and glass powder modified cement pastes were evaluated using a flow table as per ASTM C 1437. The normalized flow values (ratio of flow values of the modified pastes to that of the plain paste) for a w/s of 0.42 are shown in Fig. 2. An increase in glass powder content leads to increased flow. This is because the glass powder does not absorb any water, thereby increasing the free water content in the system. The increased workability as a result of the addition of glass powder can be beneficially employed to reduce the w/c for a specified workability, and consequently a reduction in cement content. A lower w/c improves the mechanical and durability characteristics while the reduced cement content controls thermal and shrinkage stresses.

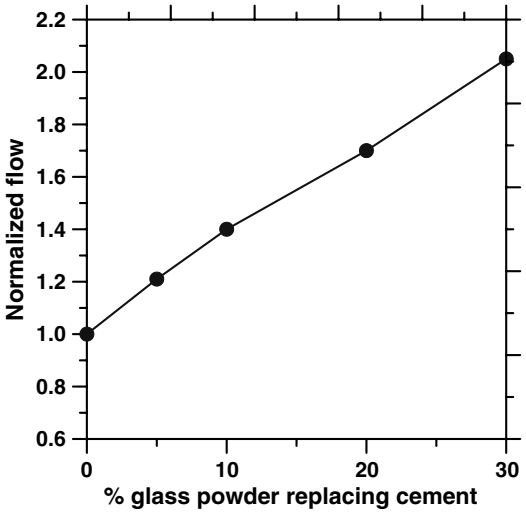

Fig. 2. Relationship between normalized flow and glass powder content (pastes with w/s 0.42).

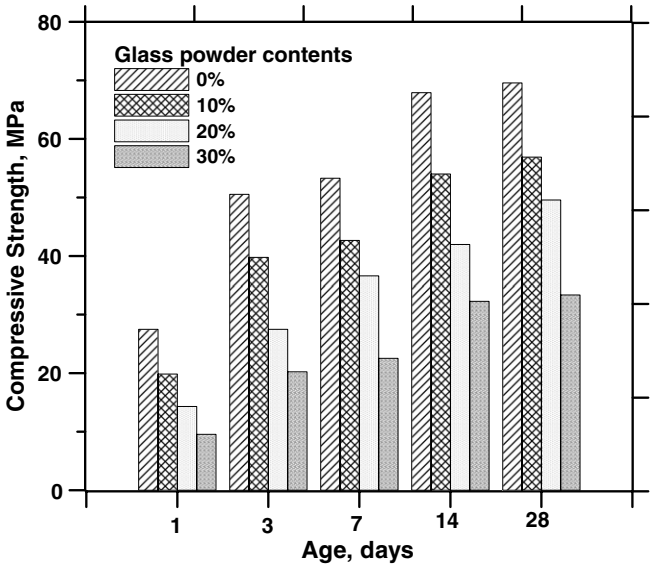

Fig. 3. Compressive strength of glass powder modified pastes (w/s 0.42).

Fig. 3 depicts the compressive strengths of glass powder modified cement pastes at various ages, determined in accordance with ASTM C 109. The compressive strengths decrease with increase in glass powder content, the reasons being the reduction in cement content and increase in effective w/c, which increases the porosity. The compressive strength results indicate no secondary reaction and strength gain. This is expected, considering the particle size range of the glass powder used in this study.

3.2. Influence of coarse glass powder on the degree of hydration of pastes

Fig. 4(a) and (b) shows the actual degrees of hydration α_{act} (or, in other words, the degree of hydration of the active particles) as determined by the method explained earlier for glass powder modified cement pastes with w/s of 0.32 and 0.42, respectively. For both w/s, replacing certain proportions of cement with glass powder results in an enhancement in the degree of hydration because of the increase in effective w/c. For 0.42 w/c plain cement paste, the α_{act} values are 0.35 and 0.68 at 1 and 28 days respectively, whereas they increase to 0.67 and 1.0 when 30% of cement is replaced with glass powder. For w/s of 0.32, α_{act} values at 28 days are 0.55 and 0.9, respectively, for plain paste and paste with 30% cement replaced by glass powder. The enhancement in α_{act} is noticed for all ages, and it increases with increase in glass powder content.

However, a high value of α_{act} does not indicate an increase in the volume of total hydration products, as is evident from the reduced compressive strengths of the glass powder modified pastes. The replacement of cement grains by the coarse glass powder causes a dilution effect. Determining the proportion of glass powder (or any inert filler) that will adequately compensate the dilution effect through an increase in α_{act} is important to attain equal or superior mechanical properties to that of the plain paste. Such an approach is beyond the scope of this paper, which deals with the estimation of microstructural development of plain and modified cement pastes using electrical properties.

3.3. Electrical conductivity as an indicator of microstructure development

Among several techniques that allow continuous monitoring of the evolution of microstructure of cement based materials, electrical property measurements have received considerable attention in the past [15–19]. The cement paste is electrically conductive by virtue of its interconnected pore network filled with water containing ions released from the cement. During hydration, the volume and connectivity of the pore network, as well as the

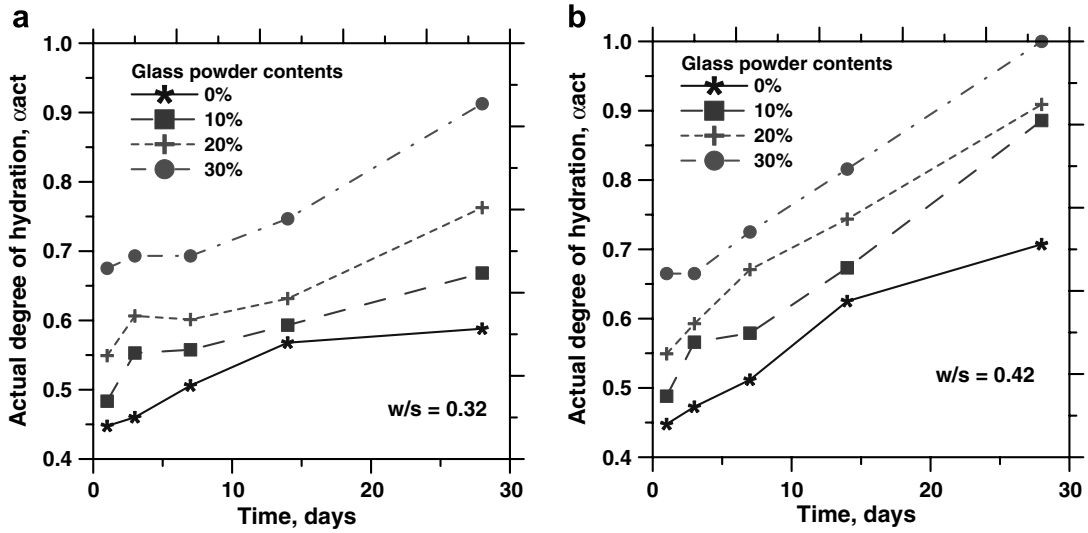

Fig. 4. Actual degrees of hydration as a function of time for glass powder modified pastes (a) w/s 0.32, (b) w/s 0.42.

conductivity of the ionic pore solution changes with time. Such a behavior allows the use of electrical conductivity as a tool to monitor microstructural changes with time. Obtaining an understanding of the continuously evolving pore structure is vital to all performance characteristics of cement based materials including strength, volumetric stability, transport characteristics, and durability. Of the electrical property based test methods, EIS which employs alternating currents at very low voltages over a range of frequencies from Hz to MHz is widely used. Details on EIS measurements to characterize cement based materials have been extensively reported [16–24].

3.4. Interpreting electrical conductivity changes with time for plain cement pastes

The variation in effective conductivity (σ_{eff}) with time for plain cement pastes having w/c of 0.32 and 0.42 are shown in Fig. 5. The secondary *Y*-axis of this plot depicts the variation in the time derivative of conductivity $\left(\frac{d\sigma_{eff}}{dt}\right)$. This was determined from the experimental conductivity–time data using a commercial software SigmaPlot™. It has to be noted here that the peaks in the effective conductivity plot do not coincide with the zero value for the derivative since the time is plotted in the log scale (in this case, the slopes of the conductivity curves are not the derivatives).

The effective conductivity increases slightly for a short period of time after mixing of cement and water, due to the dissolution of conductive ions from the cement [25–27]. The magnitude of the conductivity peak increases with increase in w/c, which can be attributed to the larger volume of conductive pore solution. The conductivity reaches a maximum, and then starts to decrease at some point in time as the water is replaced by hydration products. The first minimum in the derivative plot, indicated as 'A' in Fig. 5, can be thought of as relating to the end of dominant dissolution of ions from cement into the pore solution, i.e., the induction period. For both w/c cement pastes, the first minimum occurs at 1.44 h. The first maximum in the derivative plot (indicated as 'B') can be related to the beginning of the setting of the cement. The set time is determined by the point at which the solid phase within the microstructure begins to get connected, or the pore structure begins to depercolate, as is evident from the rapid drop in conductivity corresponding to the peak B in the $\frac{d\sigma_{eff}}{dt}$ plot. This occurs at about 3 h for the pastes shown in Fig. 5. The measured initial setting times agree with this value. The final setting time and the onset of hardening occurs between the first maximum ('B') and the second minimum ('C'). The fall in $\frac{d\sigma_{eff}}{dt}$ between 'B' and 'C' coincides with the acceleration phase in the heat evolution curve. These stages have been identified in [27] using the resistivity of hydrating cement pastes. Beyond C, which happens at about 10–12 h for the pastes shown in Fig. 5, $\frac{d\sigma_{eff}}{dt}$ increases rapidly, and the portion of the curve till the point 'D' corresponds to the deceleration stage. During this stage, the pore network becomes less and less electrically connected and the reaction is completely diffusion controlled. Beyond 'D', $\frac{d\sigma_{eff}}{dt}$ is relatively stable at or very close to 0 around and after 24–30 h, indicating that the conductivity decrease is very gradual. This (near) steady state corresponds to the one in the heat evolution curve also. However, microstructural changes are still occurring in the cement paste even after this time, but the change in conductivity is not as drastic as at early ages. This is because the solid phase in the microstructure has percolated to a sufficient degree at this time. Theoretically, conductivity measurements should be able to characterize the paste microstructure until the percolation threshold of approximately 18% has reached, beyond which the capillary pores no longer control the conductivity of the cement paste. This corresponds to a degree of hydration of approximately 0.75 for a 0.45 w/c paste [28]. Table 2 summarizes the different regions in the derivative plot in Fig. 5 with respect to its characteristics, relevant properties, and the corresponding stages in the heat evolution curve.

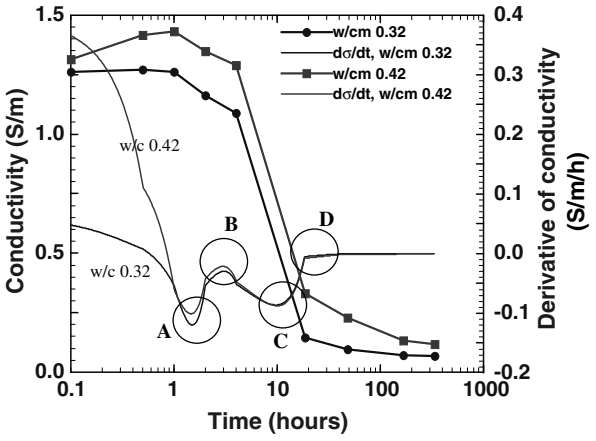

Fig. 5. Electrical conductivity and its derivative as a function of time for plain cement pastes.

3.5. Electrical conductivity response of glass powder modified pastes

The influence of cement replacement by glass powder on the electrical conductivity (σ_{eff}) and its time derivative $\left(\frac{d\sigma_{eff}}{dt}\right)$ of cement pastes made with a w/s of 0.42 is shown in Fig. 6. Similar curves were obtained for mixtures with w/s of 0.32 also. The following sub-sections describe the effective conductivity response of the glass powder modified pastes at early and later times, and also the interpretation of the time derivative plots of effective conductivity.

3.5.1. Effective conductivity at very early times (till 6–8 h)

Immediately after mixing and at very early times, the glass powder modified pastes exhibit a lower σ_{eff} than that of the plain cement paste, the lowest being observed for the mixture with the highest amount of glass powder. This could be attributed to the reduction in the amount of mobile ions released by the particulate phases soon after

Table 2
Summary of the distinct regions in the derivative plots and relevant properties

Region in the $d\sigma/dt$ curve	Approx. time range	Characteristics of $d\sigma/dt$	Relevant properties	Corresponding stage in heat evolution curve
Till A	~1.5 h	Drop in $d\sigma/dt$; goes from + to − values	σ increases, attains maximum value	Dissolution, induction
A to B	1.5–3 h	$d\sigma/dt < 0$	σ starts to decrease; beginning of setting at peak B	End of induction phase
B to C	3–10 h	$d\sigma/dt < 0$; becomes more negative	Initial and final setting occurs, hydrated products form, σ decrease rapid	Acceleration stage
C to D	10–24 h	$d\sigma/dt$ increases, but stays <0	σ decrease more gradual, diffusion controlled	Deceleration stage
Beyond D	>24 h	$d\sigma/dt \approx 0$	Slow and steady reduction in σ	Steady state

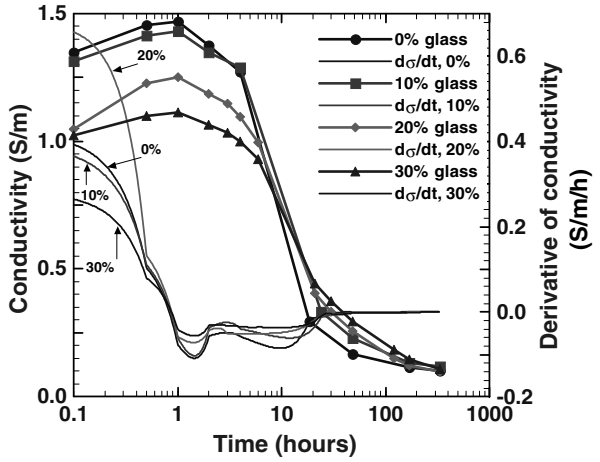

Fig. 6. Electrical conductivity and its derivative as a function of time for glass powder modified pastes (w/s 0.42).

mixing with water because of the reduced cement content. Although the alkali content of the glass powder is very high as seen from Table 1, Na^+ ions are not being released into the pore solution immediately after coming into contact with water. Measurement of conductivity of distilled water and simulated pore solution incorporating glass powder showed that the conductivity values start to increase slightly only after about 2 h, and a gradual increase is noted later on.

The value of σ_{eff} for all the mixtures increases till about 1.5 h and then starts to decrease as can be seen from Fig. 6. At points of highest conductivity, the mixture with 30% glass powder replacing cement shows a 30% lower σ_{eff} than the plain cement paste. The reasons for this could be either or both of the following: (i) the effect of reduced concentration of mobile ions as described earlier, resulting in a reduced pore solution conductivity (σ_{pore}) and (ii) the glass powder has a lower relative density than cement; therefore for a given mass replacement, there is more volume of glass powder in the mixture than the volume of replaced cement, consequently leading to a lower pore volume (ϕ_{pore}). However it needs to be emphasized here that the reduced porosity at such an early time should not be construed as an indication of lower porosity at later times. As hydration proceeds, the glass powder remains as filler, thus reducing the volume of hydrated products and consequently increasing the porosity. This is proved in Section 3.6.2 from the calculations for capillary pore volume from the actual degrees of hydration as well as by using a simplified model.

3.5.2. Effective conductivity at later times (beyond 6–8 h)

The rate of decrease of σ_{eff} between 6–8 and 24 h is highest for the plain cement paste and it decreases with increase in glass powder content, as observed in the σ_{eff}–time plots in Fig. 6. The cement content is reduced with increase in glass powder content, and since the glass powder is not expected to participate in the hydration reaction, the amount of solid hydration products is less for modified pastes, resulting in higher σ_{eff}. At ages of 24 h and beyond, the glass powder modified mixtures show higher σ_{eff} than the plain paste, and eventually at 14 days, the σ_{eff} values of plain and modified pastes are almost equal. A different approach to look at the variation in σ_{eff} at later times is given in Section 3.5.4 using normalized conductivity.

3.5.3. Interpreting the time derivative plot of conductivity

The first minimum (point A) in the derivative plot in Fig. 6 appears at about 1.5 h for all the pastes. This shows that the dissolution of ions from the cement ends at the same time irrespective of the glass powder content. However, there are discernible differences in both the σ_{eff} values as well as the magnitude of the minimum at this time. The σ_{eff} values are reduced with increase in glass powder content, and lower the glass powder content, the minimum in the derivative curve is more negative. The first maximum in the derivative curve which indicates the onset of setting is observed between 2.5 and 3 h for all the mixtures. With an increase in glass powder content, the maximum is shifted to slightly earlier periods, showing that the mixture begins to set earlier, which may possibly be attributed to the alkali activation as a result of the high alkali contents in glass powder. The second minimum is observed to occur at 9.6 h for the plain cement paste. The corresponding values are 9.8 h, 9.9 h, and 9.5 h for mixtures where 10%, 20%, and 30% cement, respectively, has been replaced with glass powder. The magnitudes of the second minima also follow a similar pattern as that of the first minima – the dips being less conspicuous with increase in glass powder content. The specific values of σ_{eff} and $\frac{d\sigma_{eff}}{dt}$ pertaining to the distinct

Table 3
Distinct regions in the conductograms and their values for pastes with w/s 0.42

Proportion of glass powder (% by mass of cement)	Point A			Point B			Point C		
	Time, h	Cond. (σ_{eff}), S/m	$\frac{d\sigma_{eff}}{dt}$, S/m/h	Time, h	Cond. (σ_{eff}), S/m	$\frac{d\sigma_{eff}}{dt}$, S/m/h	Time, h	Cond. (σ_{eff}), S/m	$\frac{d\sigma_{eff}}{dt}$, S/m/h
0	1.44	1.42	−0.110	2.96	1.25	−0.052	9.61	0.70	−0.085
10	1.44	1.38	−0.104	2.95	1.24	−0.022	9.81	0.68	−0.061
20	1.44	1.22	−0.077	2.61	1.17	−0.038	9.90	0.75	−0.047
30	1.43	1.08	−0.059	2.55	1.05	−0.015	9.51	0.73	−0.038

regions in Fig. 6 for all the pastes are shown in Table 3. Comparing the times in the derivative plot when the characteristic features appear (Table 3), it could be concluded that the incorporation of glass powder in cement pastes has a slight influence on the initial setting times, but the onset of other processes remain relatively unaffected.

3.5.4. Analysis of normalized conductivity of modified pastes

In this section, variations in normalized conductivity are explored for glass powder modified pastes. Normalized conductivity, σ_{norm}, is defined as the ratio of effective conductivity of pastes with varying amounts of glass powder at a certain time to that of plain cement paste at the same time. Fig. 7(a) and (b) shows the variation of σ_{norm} with time for mixtures with w/s of 0.32 and 0.42, respectively. These plots are useful in explaining some of the finer details beyond 6–8 h that are not very obvious from Fig. 6. At early times (less than 6–8 h), σ_{norm} is lower than 1.0 for mixtures with higher glass powder content. Two plausible reasons for this were discussed in Section 3.5.1. This trend is reversed at about 6–8 h, and at 48 h (2 days), σ_{norm} of the paste with the highest cement replacement by glass powder is the highest. This observation may be related to changes in microstructural parameters (porosity, pore solution conductivity, and pore connectivity) that result in a higher σ_{eff}, and consequently higher σ_{norm} for the modified pastes.

At 336 h (14 days), the pastes with higher amounts of glass powder show σ_{norm} values very close to 1.0. Though a greater degree of hydration of the available cement grains in modified pastes (Fig. 4) might have played some role in this, it is believed that an analysis of all parameters that contribute to σ_{eff} is required to properly understand the reasons behind such a behavior. This is attempted in this paper using a parallel model, which is one of the common models to describe the effective conductivity of cement based materials [29]. For cement pastes, σ_{eff} can be expressed in terms of the conductivity of the pore solution (σ_{pore}), the pore volume fraction (ϕ_{pore}), and the pore connectivity factor (β) as

$$\sigma_{eff} = \sigma_{pore}\phi_{pore}\beta \quad (4)$$

The following section evaluates these parameters in greater detail.

3.6. Estimating the pore solution conductivity and microstructural parameters

3.6.1. Influence of glass powder addition on the conductivity of pore solution

Since the pore solution is the electrically conducting phase in cement pastes, it is necessary to estimate the conductivity of the pore solution (σ_{pore}) in order to be able to

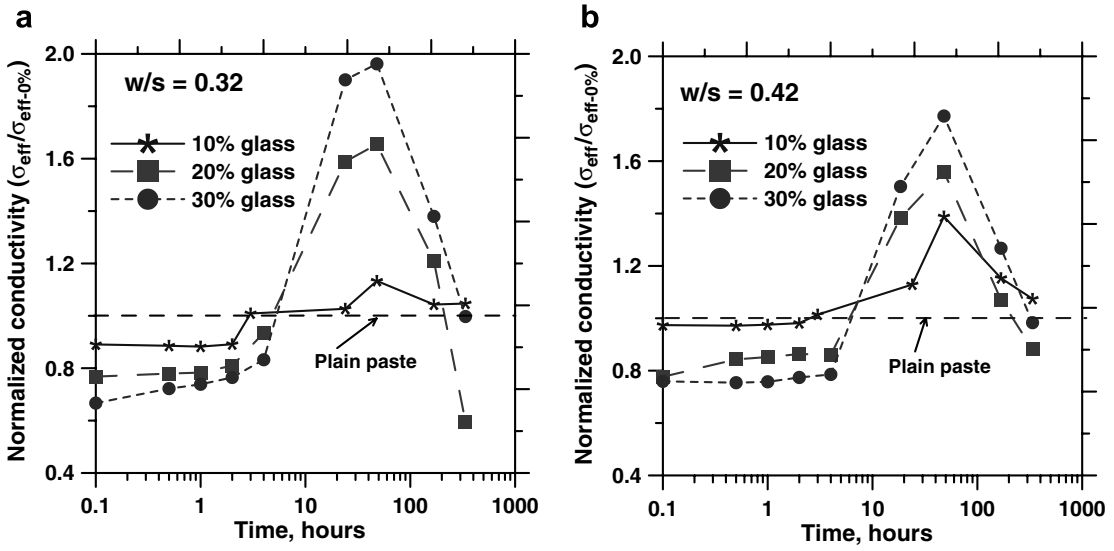

Fig. 7. Variation of normalized conductivity with time for glass powder modified cement pastes (a) w/s 0.32, (b) w/s 0.42.

use models for prediction of σ_{eff}. Experimental methods of pore solution analysis by squeezing the pore solution from hardened pastes have been reported and practiced [25,30]. In this paper, σ_{pore} is determined using an indirect method. The concentrations of the dominant ions (Na^+, K^+, and OH^-) in 1 day or older pastes are calculated using the procedure outlined by Taylor [31], which has been found to predict these concentrations fairly accurately. Using the concentrations of the ionic species obtained from Taylor's models, σ_{pore} can be estimated using Eq. (5) [32]

$$\sigma_{pore} = \sum \frac{z_i \lambda_i^0 c_i}{1 + G_i I_M^{0.5}} \quad (5)$$

where z_i is the valence, λ_i^0 is the equivalent conductivity at infinite dilution, the values of which are given in [32], c_i is the molar concentration determined using Taylor's model, and G_i is an empirical coefficient, all for the species i. I_M is the ionic strength on a molar basis given by

$$I_M = \frac{1}{2} \sum z_i^2 c_i \quad (6)$$

Fig. 8(a) and (b) illustrates the variation in the concentration of Na^+, K^+, and OH^- with glass powder contents at 2 and 14 days, respectively. These two times are chosen here because σ_{norm} attains a maximum value at 2 days, and then approaches a value of 1.0 at 14 days, as can be seen from Fig. 7(a) and (b). At both these times, the Na^+ concentration increases with increase in glass powder content because of the higher Na_2O content in the glass powder. The K^+ concentration is found to decrease with increasing glass powder content, due to the lower K_2O content in glass powder than the cement it replaces. At 14 days, the Na^+ concentration in the pore solution rises at a much faster rate with glass powder content than at 2 days. Since glass powder is an inert filler, the volume of hydration products is less in modified pastes, leading to a reduction in the amount of ions that can be incorporated into the hydration products. Majority of these ions thus remain in the pore solution. The OH^- ion concentration does not show any appreciable change with increase in glass powder content at 2 days, whereas at 14 days, it increases. The reason for this behavior is the following. The OH^- concentration is determined from charge balance as [31]: $c_{OH^-} = c_{Na^+} + c_{K^+}$. From Fig. 8(a), at 2 days, it can be seen that an increase in Na^+ concentration is more or less balanced by a reduction in K^+ concentration, thus leading to no significant change in the OH^- concentration. From Fig. 8(b), at 14 days, the Na^+ concentration increases at a faster rate than the reduction in K^+ concentration with glass powder addition, resulting in an increase in OH^- concentration.

The values of σ_{pore} estimated using Eq. (5) are shown in Fig. 9. It is seen that σ_{pore} is higher at 14 days than 2 days for all the pastes, which is in agreement with previous findings that the pore solution conductivity increases with time at least until 28 days [16,25,31]. With increase in glass powder content, σ_{pore} stays fairly constant at 2 days because of the near constant OH^- concentration (Fig. 8(a)) which is the dominant contributor to σ_{pore}. σ_{pore} is found to increase with glass powder content at 14 days, which is the consequence of increasing OH^- and Na^+ concentrations. It can be seen from Fig. 9 that the incorporation of glass powder in cement pastes leads to drastic increase in σ_{pore} at later ages. The aforementioned reason, combined with the reduction in volume of hydration products that can sorb the alkali ions result in such high values of σ_{pore}.

3.6.2. Estimating the capillary porosity

Using the actual degrees of hydration (α_{act}), the capillary porosity (ϕ_{pore}) of the plain and modified pastes were determined using Eq. (7) [33]

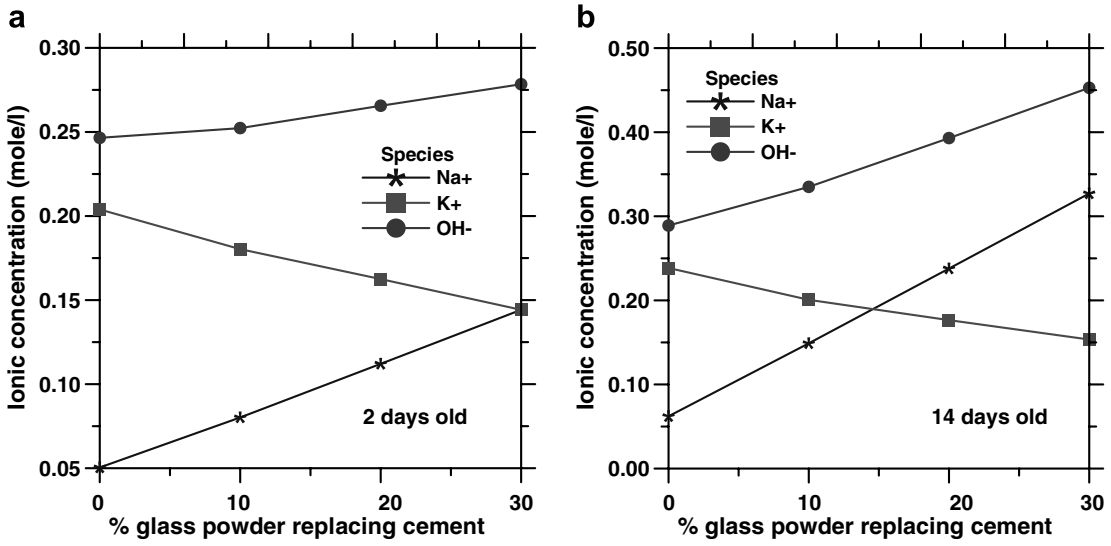

Fig. 8. Variation of ionic concentration in the pore solution with glass powder content for w/s 0.42 pastes, computed from Taylor's model (a) at 2 days, (b) at 14 days.

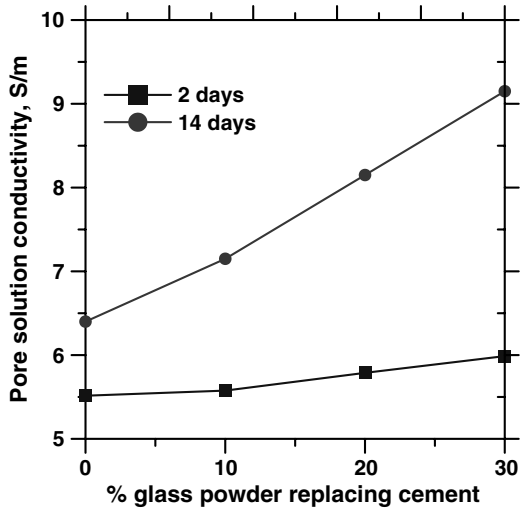

Fig. 9. Pore solution conductivity as a function of glass powder content (pastes with w/s 0.42).

$$\phi_{\text{pore}} = \frac{\rho_{\text{cem}}(\text{w/c})_{\text{eff}} - f_{\text{exp}}\alpha_{\text{act}}}{1 + \rho_{\text{cem}}(\text{w/c})_{\text{eff}} + \frac{\rho_{\text{cem}}}{\rho_{\text{glass}}}(\text{g/c})} \quad (7)$$

ρ_{cem} and ρ_{glass} are the specific gravities of the cement (3.15) and glass powder (2.50) respectively, f_{exp} is the volumetric expansion coefficient for the solid cement hydration products relative to the cement ($2.15 - 1 = 1.15$), and g/c is the glass powder to cement ratio by mass. $(\text{w/c})_{\text{eff}}$ is the effective water–cement ratio, which for a w/s of 0.42% and 20% replacement of cement by glass powder, is 0.525.

Fig. 10 depicts the variation in porosity with glass powder content for pastes with w/s of 0.42 at 2 days and 14 days. Immediately after mixing with water, and at very early ages, the local porosity reduces with increase in inert glass powder filler content because of the lower relative density of the glass powder as compared to that of cement. However, as hydration proceeds, the porosity increases with increase in glass powder content, as can be observed

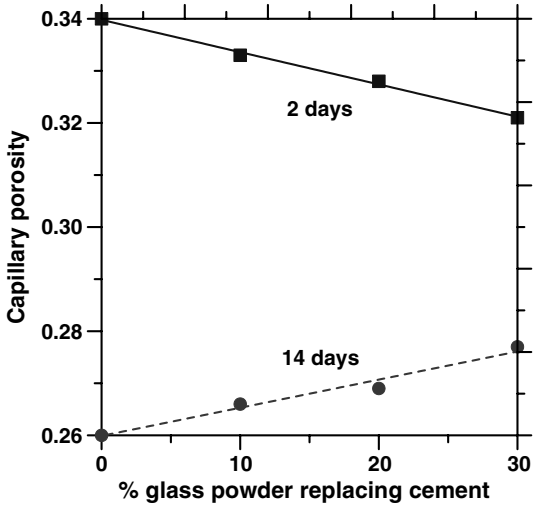

Fig. 10. Capillary porosity as a function of glass powder content (pastes with w/s 0.42).

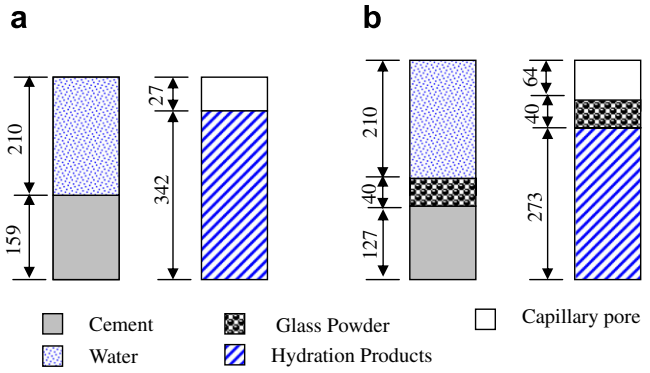

Fig. 11. Schematic illustration of the volume of the constituents, hydrated products, and capillary pore (a) plain cement paste, (b) 20% cement replaced with glass powder (the numbers are the volumes in cc).

for 14 day old pastes. This can be illustrated by the following simple model, depicted in Fig. 11. Consider 500 g of cement mixed with 210 g of water (w/c 0.42) as shown in Fig. 11(a). The original volume of cement in the paste is 159 cc (500/3.15), and that of water is 210 cc, providing a total volume of 369 cc. After the cement has completely hydrated, it occupies 2.15 times the original volume, i.e., 342 cc, leaving 27 cc or 7.3% as capillary porosity. If 20% by mass of cement is replaced with glass powder having a specific gravity of 2.50, as shown in Fig. 11(b), the volumes of cement, glass powder and water in the paste are 127 cc, 40 cc, and 210 cc, respectively. After complete hydration of the cement, the volume of hydrated products then is 273 cc. Since the glass powder is only a filler, this leaves a pore volume of 64 cc or 17%.

3.6.3. Determination of pore connectivity factor (β) from effective conductivity

The values of σ_{eff} experimentally obtained using Eq. (1), ϕ_{pore} calculated using Eq. (7), and σ_{pore} at 2 days and 14 days determined using the procedure explained in Section 3.6.1 are used to determine the pore connectivity factor (β) using Eq. (4) and plotted in Fig. 12 as a function of the glass powder content. β increases with increase in glass powder content at 2 days. This explains the reason for a higher σ_{eff} (and thus, σ_{norm} as seen in Fig. 7) at 2 days for the glass powder modified pastes even when ϕ_{pore} is lower (Fig. 10) and σ_{pore} is fairly constant (Fig. 9). At 14 days, σ_{norm} is close to 1.0 (i.e., σ_{eff} of the plain and modified pastes are very close to each other), even when ϕ_{pore} and σ_{pore} are significantly higher for the modified pastes (Figs. 9 and 10). The σ_{eff} of the modified pastes is lowered by a reduction in β to bring σ_{norm} close to 1.0. At relatively later ages (14 days), a combination of higher degrees of hydration of the available cement grains (Fig. 4), and the presence of a higher volume of unreacted particles of the glass powder than the cement it replaced (because of the lower specific gravity of the filler), modifies the pore structure of the material so as to make the electrical conduction paths more tortuous, demonstrated by a reduction in β. It

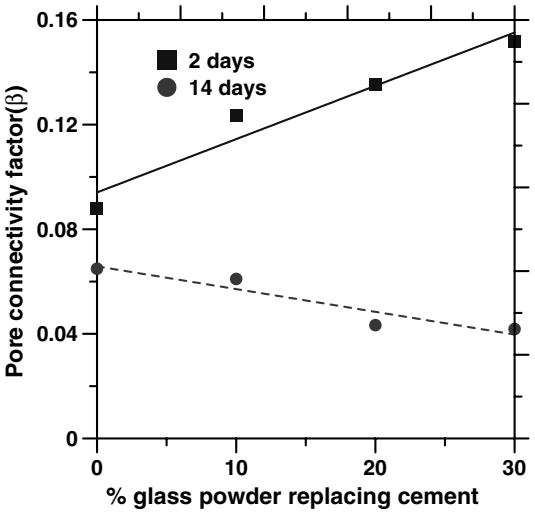

Fig. 12. Variation of pore connectivity factor with glass powder content (pastes with w/s 0.42).

is important to note here that the reduction in β does not imply increased volume of hydration products as compared to the plain paste.

4. Conclusions

This paper has dealt with characterization of cement pastes incorporating coarse glass powder as a filler material using effective electrical conductivity and its time derivative. The following conclusions are drawn from this study:

(i) The workability of the pastes was found to increase with glass powder addition because of the increase in effective w/c and the negligible water absorption of the glass powder. This characteristic can be beneficially employed to reduce the w/c for a given workability, and thus the cement content. Replacing a certain portion of cement by coarse glass powder results in reduced compressive strengths of the paste because of the increase in effective w/c as well as the dilution effect which reduces the volume of hydration products. The actual degree of hydration of the cement grains also increases with glass powder addition. For the glass powder contents investigated in this study, the effect of dilution is more than what could be compensated by the increase in actual degree of hydration.

(ii) The variation of electrical conductivity with time and its derivative can be related to the microstructure development in cement pastes. The distinct regions in the derivative plots show correspondence to the dissolution phase, acceleration and deceleration phases, and steady state in a typical heat evolution curve.

(iii) The effective conductivity of the plain paste is higher at very early times due to the dissolution of more ions into the pore solution, where as it is lower at later times because of the formation of a less connected pore structure. The glass powder modified pastes show lower initial conductivities as a result of reduced ionic concentration, and reduced pore volume, both being direct consequences of the reduction in cement content. From the derivative plots, it was observed that the replacement of cement by glass powder in the proportions used in this paper results in only slight changes in the initial setting time.

(iv) The Na^+ concentration increases with increase in glass powder content in the paste, due to the higher Na_2O content in the glass powder. The K^+ concentration decreases because the glass powder has lesser amount of K_2O than the cement it replaces. At 2 days, the increase in Na^+ is compensated by the reduction in K^+, resulting in no significant changes in pore solution conductivity with glass powder addition. However, at 14 days, the Na^+ concentration in the pore solution rises at a much faster rate with increasing glass powder content, consequently increasing the pore solution conductivity.

(v) At early times, local porosity reduces with increase in glass powder content because of the lower relative density of the filler as compared to that of cement. As hydration proceeds, the porosity increases with increase in glass powder content because there is insufficient hydration products as a result of the reduced cement content and the increased effective w/c.

(vi) A parallel model has been used to describe effective conductivity as a function of the pore solution conductivity, porosity, and the pore connectivity factor. At early times, the pore connectivity factor increases with increase in glass powder content, and reduces at later times (14 days). This reduction in pore connectivity factor is responsible for the lower values of normalized conductivity at later times even when the porosity and pore solution conductivity are higher. The reduction in pore connectivity factor for inert filler modified pastes has a different meaning than that of normal cementitious materials. In this case, a reduction in pore connectivity factor does not imply increased volume of hydration products as is usual, but the electrical conduction paths are believed to be made more tortuous by the presence of higher volume of unreacted filler particles (because of its lower specific gravity).

Acknowledgment

This study was conducted with financial support from Empire State Development Program of New York State, which is acknowledged.

References

[1] Taylor HFW. Cement chemistry. 2nd ed. London: Thomas Telford; 1997.

[2] Bentz DP, Haecker CJ. An argument for using coarse cements in high performance concretes. Cem Concr Res 1999;29:615–8.
[3] Bentz DP, Conway JT. Computer modeling of the replacement of "coarse" cement particles by inert fillers in low w/c ratio concretes. Cem Concr Res 2001;31:503–6.
[4] Bentz DP. Replacement of "coarse" cement particles by inert fillers in low w/c ratio concretes II. Experimental validation. Cem Concr Res 2005;35:185–8.
[5] Zhu W, Gibbs JC. Use of different limestone and chalk powders in self-compacting concrete. Cem Concr Res 2005;35:1457–62.
[6] Bonavetti V, Donza H, Menendez G, Cabrera O, Irassar EF. Limestone filler in low w/c concrete: a rational use of energy. Cem Concr Res 2003;33:865–71.
[7] Shi C, Wu Y, Riefler C, Wang H. Characteristics and pozzolanic reactivity of glass powders. Cem Concr Res 2005;35:987–93.
[8] Poppe AM, Schutter GD. Cement hydration in the presence of high filler contents. Cem Concr Res 2005;35:2290–9.
[9] Jin W, Meyer C, Baxter S. Glascrete – concrete with glass aggregates. ACI Mater J 2000;97(2):208–13.
[10] Shayan A, Xu A. Value-added utilization of waste glass in concrete. Cem Concr Res 2004;34:81–9.
[11] Chen G, Lee H, Young KL, Yue PL, Wong A, Tao T, et al. Glass recycling in cement production – an innovative approach. Waste Manage 2002;22:747–53.
[12] Xie Z, Xi Y. Use of recycled glass as a raw material in the manufacture of portland cement. Mater Struct 2002;35:510–5.
[13] Shayan A, Xu A. Performance of glass powder as a pozzolanic material in concrete: a field trial on concrete slabs. Cem Concr Res 2006;36:457–68.
[14] Shao Y, Lefort T, Moras S, Rodriguez D. Studies on concrete containing ground waste glass. Cem Concr Res 2000;30:91–100.
[15] Whittington HW, McCarter J, Forde MC. The conduction of electricity through concrete. Mag Concr Res 1981;33(114):48–60.
[16] Christensen BJ, Coverdale RT, Olson RA, Ford SJ, Garboczi EJ, Jennings HM, et al. Impedance spectroscopy of hydrating cement based materials: measurement, interpretation and application. J Am Ceram Soc 1994;77:2789–804.
[17] McCarter WJ, Starrs G, Chrisp TM. Immitance spectra for portland cement/fly ash based binders during early hydration. Cem Concr Res 1999;30:377–87.
[18] McCarter WJ, Starrs G, Chrisp TM. Electrical conductivity, diffusion, and permeability of Portland cement-based mortars. Cem Concr Res 2000;30:1395–400.
[19] Dotelli G, Mari CM. The evolution of cement paste hydration process by impedance spectroscopy. Mater Sci Eng A 2001;33:54–9.
[20] Neithalath N, Weiss J, Olek J. Characterizing enhanced porosity concrete using electrical impedance to predict the acoustic and hydraulic performance. Cem Concr Res 2006;36:2074–85.
[21] Gu P, Xu Z, Xie P, Beaudoin JJ. Application of A.C. impedance techniques in studies of porous cementitious materials – (I) Influence of solid phase and pore solution on high frequency resistance. Cem Concr Res 1993;23:531–40.
[22] Ford SJ, Mason TO, Christensen BJ, Coverdale RT, Jennings HM. Electrode configurations and impedance spectra of cement pastes. J Mater Sci 1995;30:1217–24.
[23] Moss GM, Christensen BJ, Mason TO, Jennings HM. Microstructural analysis of young cement pastes using impedance spectroscopy during pore solution exchange. Adv Cem Based Mater 1996;4:68–75.
[24] Schießl A, Weiss WJ, Shane JD, Berke NS, Mason TO, Shah SP. Assessing the moisture profile of drying concrete using impedance spectroscopy. Concr Sci Eng 2000;2:106–16.
[25] Christensen BJ. Microstructure studies of hydrating Portland cement based materials using impedance spectroscopy. Ph.D Thesis, Northwestern University, 1993.
[26] Salem ThM. Electrical conductivity and rheological properties of ordinary portland cement-silica fume and calcium hydroxide-silica fume pastes. Cem Concr Res 2002;32:1473–81.
[27] Li Z, Wei X, Li W. Preliminary interpretation of portland cement hydration process using resistivity measurements. ACI Mater J 2003;100(3):253–7.
[28] Bentz DP, Garboczi EJ. Percolation of phases in a three-dimensional cement paste microstructure model. Cem Concr Res 1991;21:325–44.
[29] Garboczi EJ. Permeability, diffusivity and microstructural parameters: a critical review. Cem Concr Res 1990;20:591–601.
[30] Barneyback RS, Diamond S. Expression and analysis of pore fluid from hardened cement pastes and mortars. Cem Concr Res 1981;11:279–85.
[31] Taylor HFW. A method for predicting alkali ion concentrations in cement pore solutions. Adv Cem Res 1987;1:5–17.
[32] Snyder KA, Feng X, Keen BD, Mason TO. Estimating the conductivity of cement paste pore solutions for OH^-, K^+ and Na^+ concentrations. Cem Concr Res 2003;33:793–8.
[33] Bentz DP. Influence of water-to-cement ratio on hydration kinetics: simple models based on spatial considerations. Cem Concr Res 2006;36:238–44.